Reduced Complexity Digital Back-Propagation Methods for Optical Communication Systems

Antonio Napoli, Zied Maalej, Vincent A. J. M. Sleiffer, *Student Member, IEEE*, Maxim Kuschnerov, Danish Rafique, Erik Timmers, Bernhard Spinnler, Talha Rahman, *Student Member, IEEE*, Leonardo Didier Coelho, *Member, IEEE*, and Norbert Hanik, *Member, IEEE*

***Abstract*—Next-generation optical communication systems will continue to push the (*bandwidth · distance*) product towards its physical limit. To address this enormous demand, the usage of digital signal processing together with advanced modulation formats and coherent detection has been proposed to enable data-rates as high as 400 Gb/s per channel over distances in the order of 1000 km. These technological breakthroughs have been made possible by full compensation of linear fiber impairments using digital equalization algorithms. While linear equalization techniques have already matured over the last decade, the next logical focus is to explore solutions enabling the mitigation of the Kerr effect induced nonlinear channel impairments. One of the most promising methods to compensate for fiber nonlinearities is digital back-propagation (DBP), which has recently been acknowledged as a universal compensator for fiber propagation impairments, albeit with high computational requirements. In this paper, we discuss two proposals to reduce the hardware complexity required by DBP. The first confirms and extends published results for non-dispersion managed link, while the second introduces a novel method applicable to dispersion managed links, showing complexity reductions in the order of 50% and up to 85%, respectively. The proposed techniques are validated by comparing results obtained through post-processing of simulated and experimental data, employing single channel and WDM configurations, with advanced modulation formats, such as quadrature phase shift keying (QPSK) and 16-ary quadrature amplitude modulation (16-QAM). The considered net symbol rate for all cases is 25 GSymbol/s. Our post-processing results show that we can significantly reduce the hardware complexity without affecting the system performance. Finally, a detailed analysis of the obtained reduction is presented for the case of dispersion managed link in terms of number of required complex multiplications per transmitted bit.**

***Index Terms*—Advanced modulation formats, coherent detection, digital signal processing(DSP), nonlinear mitigation.**

I. Introduction

OVER the last decade, communication traffic showed an exponential growth [1]. This trend has lately been supported by the introduction of new multimedia services, such as cloud computing, video streaming, and social networks, essentially pushing currently available transmission capacity to its limits [2].

Due to the aforementioned stringent capacity demands, the legacy networks employing 10 Gb/s on-off keying (OOK) traffic are not able to fuel the needs of state-of-the-art multimedia applications. Consequently, over the past few years research has intensified on optical systems based on transceivers employing coherent detection and digital signal processing (DSP), together with phase and amplitude modulated formats such as binary phase shift keying, quadrature phase shift keying (QPSK) or quadrature amplitude modulation (e.g., 16-QAM) [3]–[5].

In particular, the recent application of DSP to optical communications has moved the balance of system complexity from the transmission link to the end nodes. With current technological advancements, modern DSP-based coherent receivers (DSP-CRX)[1] are able to fully compensate for linear channel impairments, such as chromatic dispersion (CD) and polarization mode dispersion (PMD) [4]. Consequently, the transmission performance remains ultimately limited by nonlinear fiber effects [6]. For this purpose different nonlinear compensation methods have been proposed and investigated to reduce the impact of Kerr induced nonlinearities. Among them Volterra series based equalizer [7], radio-frequency (RF)-pilot tone technique [8], [9], phase-conjugated twin waves [10] and eventually the digital back-propagation algorithm (DBP) [11] are worth to be mentioned. DBP has recently gained a momentum [11]–[14], and it is now commonly acknowledged as one of the most suitable candidates for joint compensation of linear and nonlinear effects. In particular, fiber impairments such as self-phase modulation (SPM), cross-phase modulation (XPM) and four-wave mixing represent the bottle-neck for future optical transport networks, capable to transmit data-rates as high as 400 Gb/s per channel with a high spectral efficiency over distances of about 1000 km [5], [15]. Theoretically, DBP can compensate for any deterministic nonlinear effect, however practically, due to

Manuscript received September 14, 2013; revised December 4, 2013 and December 23, 2013; accepted January 1, 2014. Date of publication January 19, 2014; date of current version March 3, 2014.

A. Napoli, M. Kuschnerov, D. Rafique, B. Spinnler, and L. D. Coelho are with Coriant R&D GmbH, Munich 81541, Germany (e-mail: antonio.napoli@coriant.com; maxim.kuschnerov@coriant.com; danish.rafique@corian.com; bernhard.spinnler@coriant.com; leonardo.coelho@ieee.org).

Z. Maalej was with Technische Universität München, Munich 85748, Germany. Now he is with Vodafone Deutschland, Munich (e-mail: zied.maalej@vodafone.com).

V. A. J. M. Sleiffer and T. Rahman are with the Eindhoven University of Technology, Eindhoven, The Netherlands (e-mail: v.a.j.m.sleiffer@tue.nl; t.rahman@tue.nl).

E. Timmers was with Eindhoven University of Technology, Eindhoven, The Netherlands. He is now with easyGIS, Eindhoven, The Netherlands (e-mail: etimmers@gmail.com).

N. Hanik is with the Institute for Communications Engineering, Technische Universität München, Munich 80290, Germany (e-mail: norbert.hanik@tum.de).

Color versions of one or more of the figures in this paper are available online at http://ieeexplore.ieee.org.

Digital Object Identifier 10.1109/JLT.2014.2301492

[1]Hereafter, only intra-dyne coherent receivers are considered.

hardware requirements, its usage is limited to the information of a single channel, implying that only intra-channel effects such as SPM may be effectively compensated by DBP [16].

Long-haul optical communication systems can be divided in two macro categories, according to the method of managing dispersion: non-dispersion managed (NDM) and dispersion managed (DM). In case of NDM systems there is no in-line dispersion compensation, and the equalization of propagation effects has been completely moved to the DSP-CRX. In this context, effects such as SPM and XPM equally affect the transmission performance, provided that only phase modulation formats are transmitted [5], [17]. In this scenario, DBP can effectively contribute to increase the (*bandwidth* · *distance*) product. On the other hand, DM systems are characterized by an accurate dispersion map design, to increase the tolerance against linear and nonlinear effects, and they are mainly limited by inter-channel nonlinearities (e.g. XPM). These systems present their worst case scenario whenever neighboring channels are OOK [18]. Alfiad *et al.* showed in [19] that NDM links represent a better solution for next generation optical communication systems employing DSP-CRX, nevertheless a crucial feature of modern transponders will be their performance applied to legacy links (e.g., DM systems) which constitute the vast majority of the currently deployed links. At the time of writing, optical communication systems have been mostly employed to transmit data-rate as low as 10/40 Gb/s, with rare cases of upgrades to 100 Gb/s [3], [5]. Now, network operators urgently need to increase the transmitted data-rate per channel to fulfill the required bandwidth of nowadays applications. In this context, the possibility of effectively re-using legacy links will play a considerable role in terms of cost reduction, avoiding greenfield deployment. The aforementioned upgrade will suffer limitations in performance due to strong intra- and inter-channel nonlinear effects. The mitigation of intra-channel nonlinearities through DSP-CRX, employing reduced complexity DBP, represents the goal of this study.

Throughout this article, we utilize DBP to compensate for the bulk accumulated dispersion and intra-channel nonlinear effects (i.e., SPM) for both NDM and DM systems. The equalization of the residual linear effects is performed by the time domain equalizer (TDE).

The performance of DBP has been explored in detail [11]–[13], [20], however with lesser focus on the practicality of this approach. Nonetheless, few solutions have been proposed to reduce the number of DBP steps. For instance, in [21], [22], a method based on the information provided by the neighboring symbols is proposed, which reports up to 80% reductions in DBP complexity in terms of required number of steps, with the drawback of extra filter coefficient calculations. Another solution, proposed in [23], utilizes only fractions of the received spectrum, enabling improved system performance with lower hardware complexity. Indeed, the aforementioned proposals reduce the computational complexity of DBP, but they do not reach a critical point of enabling a rapid hardware implementation. This paper proposes two innovative strategies to significantly decrease the hardware complexity of the DBP method applied to NDM and DM systems.

TABLE I
FIBER PHYSICAL PARAMETERS [24]

PARAMETERS	SSMF	LA-PSCF
Attenuation α [dB/km]	0.19	0.161
Dispersion Coefficient D at 1550 nm [ps/nm/km]	16.8	21
Dispersion Slope S [ps^2/nm/km]	0.057	0.061
Effective Core Area A_{eff} [μm^2]	80	133
Nonlinear Coefficient γ [1/(W·km)]	1.14	0.6

TABLE II
CONSIDERED SYSTEM SETUPS

Scenario	type	modulation format	distance	ref.
NDM	simulation	POLMUX-16-QAM	8x82 km	[25]
NDM	experiment	POLMUX-QPSK	variable	[26]
DM	simulation	POLMUX-16-QAM	8x82 km	[25]
DM	experiment	POLMUX-QPSK	variable	[4]

In the next sections, we first show that, for the case of NDM links, an approximation of the nonlinear channel considerably reduces the number of spans needed by DBP, without significantly degrading its performance. Second, the physical design of DM links is exploited to decrease the number of needed DBP steps, maintaining the algorithm's performance. Our investigations have been validated by using both simulated and experimental data-sets, where various advanced modulation formats have been propagated by keeping the symbol rate constant at 25 GSymbol/s.

This article is structured as follows: In Section II, we describe the transmission setup (both numerical and experimental) along with standard DSP algorithm. Section III deals with the theory concerning DBP. In Section IV and V, we describe two proposed strategies for hardware complexity reduction for NDM and DM links, respectively. Section VI presents an analytical calculation of the computation reduction in terms of complex multiplications per transmitted bit for the DM scenario. Finally, Section VII summarizes the work and draws conclusions.

II. FIBER PARAMETERS AND DIGITAL COHERENT RECEIVER EMPLOYING BACK-PROPAGATION

A. Fiber Parameters and System Setups

In our study, we considered different scenarios (NDM and DM), different types of fibers (standard single mode fiber (SSMF) and large A_{eff} pure silica core fiber (LA-PSCF)), different modulation formats (16-QAM and QPSK), and different link distances.

The most relevant physical parameters of the two considered fibers are listed in Table I. We highlight that LA-PSCF is characterized by a relatively high dispersion coefficient D and a significantly low nonlinear coefficient γ.

In addition, Table II summarizes the analyzed transmission setups, which are in detail described in the references herein provided. For all four cases, we post-processed data with single channel and WDM, usually employing 200 Gb/s 16-QAM for the simulations and 100 Gb/s QPSK for the experiments. The transmitted net symbol rate was 25 GSymbol/s for all analyzed cases. In the case of the two experiments the signal was propagated over different distances: in NDM we post-processed the

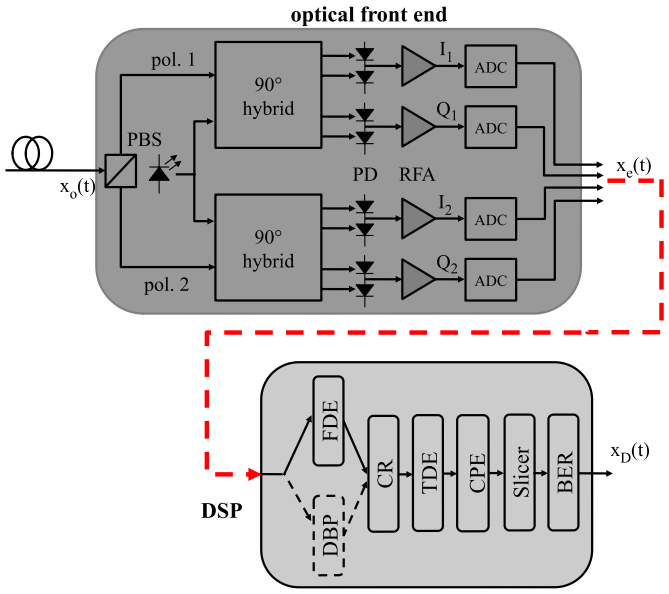

Fig. 1. Block diagram of a DSP-based coherent receiver, where the red dashed line contains the four components connecting the optical front-end to the DSP block. PBS: polarization beam splitter; PD: Photo-diode; RFA: Radio frequency amplifier.

data after 28 and 56 spans (with 1 span = 82 km); while in the DM scenario we considered different distances as described in Section V-B and in [4]. Lastly, the numerical simulations considered shorter distances due to the transmission limitations of high order modulation formats such as 16-QAM in [5].

B. Digital Coherent Receiver

The recent development of high-speed digital electronics has enabled the use of powerful DSP algorithms to compensate for several impairments at once. Within a DSP-CRX the optical phase information is preserved during the optical / electrical conversion, at the receiver front-end, where the incoming signal is superimposed with the output of a local oscillator (LO). The LO consists of a receiver-side LASER with a low linewidth and higher power compared to the detected signal, i.e., the receiver sensitivity is consequently enhanced [3].

In Fig. 1 a high level block diagram of a DSP-based polarization diversity coherent receiver is illustrated. First, a polarization beam splitter (PBS) separates the optical signal $x_o(t)$ into two arbitrary, but orthogonal, polarization components X and Y. Each of the polarization components is fed to a 90° hybrid, and afterward mixed with the LO. The mixing of the received signal and the LO in the 90° hybrids separates the in-phase and quadrature components, which are then detected by balanced photo-diodes (PD). This is followed by a radio-frequency amplifier, and four high-speed analog-to-digital converters, which represents the first element of the DSP-CRX. Following, a clock recovery, based on [27], is applied. The fiber propagation impairments are afterward compensated by using either a frequency domain equalizer (FDE) plus a TDE (upper path of Fig. 1, solid line) or by employing DBP plus TDE (lower path of Fig. 1, dashed line).

In case only linear equalization is applied (upper path in Fig. 1), FDE compensates for bulk accumulated dispersion over the whole link [28], whereas the TDE, whose coefficients are optimized through the constant modulus algorithm (CMA) [29] and the least mean square (LMS) algorithm [27], compensates for distortions such as residual dispersion, PMD and polarization dependent loss (PDL), besides realizing polarization demultiplexing of the equivalent multiple-input–multiple-output (MIMO) channel [30]. On the other hand, if the lower path is selected, bulk dispersion is compensated on a span-by-span basis by the linear part of DBP, while the nonlinear one mitigates the nonlinear fiber impairments.[2] The TDE operates exactly as for the upper path. Finally, the carrier phase estimation (CPE) cancels out the phase and frequency offset between LO and transmitter LASER. We would like to point out that the employed CPE was different for QPSK and 16-QAM case. For the first modulation format, we employed a Viterbi & Viterbi algorithm [31], while for the second a phase-locked loop (PLL) based carrier recovery as reported in [32]. The post-processing ends with the digital decision of (signal $x_D(t)$ in Fig. 1) and, if required, it is followed by a differential decoder.

III. Theory of Digital Back-propagation

A. Propagation Equations

Digital back-propagation aims at inverting, at the receiver, the optical channel of the forward propagation. An optical link consists of N spans, each made of an optical fiber described through its physical parameters, namely the attenuation α, the dispersion parameter β_2 and the nonlinear coefficient γ, as reported in Table I. Within DBP, they all assume the opposite sign with respect to the forward propagation.

The simplest approximation of the optical signal propagation is provided by the nonlinear Schrödinger equation (NLSE) [6], which reads as

$$\frac{\partial E}{\partial z} = \frac{j\beta_2}{2}\frac{\partial^2 E}{\partial t^2} - j\gamma|E|^2 E - \frac{\alpha}{2}E \tag{1}$$

where E is the electrical field and z is the propagation axis. Equation (1) represents a sufficiently precise model only for single polarization transmission [6].

To increase the spectral efficiency of an optical signal, polarization multiplexing (POLMUX) has been recently adopted. Propagation over two polarizations implies that linear and nonlinear interactions between them must be also taken into account. Consequently eq. (1) is transformed into its vectorized form as

$$\begin{aligned}\frac{\partial E_X}{\partial z} &= -\frac{\alpha}{2}E_X + \frac{j\beta_2}{2}\frac{\partial^2}{\partial t^2}E_X + \\ &\quad - j\gamma\left(|E_X|^2 + \frac{2}{3}|E_Y|^2\right)E_X - \frac{j\gamma}{3}E_X^* E_Y^2 \\ \frac{\partial E_Y}{\partial z} &= -\frac{\alpha}{2}E_Y + \frac{j\beta_2}{2}\frac{\partial^2}{\partial t^2}E_Y + \\ &\quad - j\gamma\left(\frac{2}{3}|E_X|^2 + |E_Y|^2\right)E_Y - \frac{j\gamma}{3}E_X^2 E_Y^*\end{aligned} \tag{2}$$

[2] As only the information of one channel is available, the solely SPM can be compensated for by DBP.

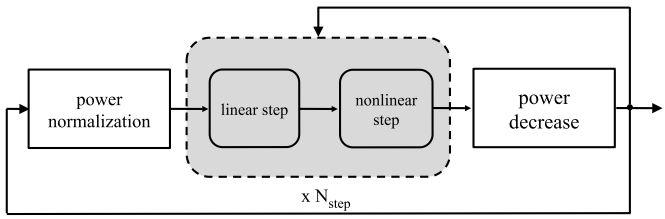

Fig. 2. Example of span block diagram for the DBP method employing the Wiener model, N_{step} is the number of steps used by the DBP algorithm.

where E_X and E_Y are the two orthogonal polarization components of the electric field E. For reasons reported in [11], [13], concerning the residual birefringence present in the fiber, we employed only the Manakov equation [6] throughout this article. In fact, since the polarization state of the electric field changes rapidly, the resulting nonlinearities do not correspond to the ones from a linearly or circularly polarized field but to an average over the entire Poincaré sphere. Averaging eq. (2) over the fast polarization changes, results into the following two Manakov equations

$$\frac{\partial E_X}{\partial z} = \underbrace{-\frac{\alpha}{2}E_X + \frac{j\beta_2}{2}\frac{\partial^2}{\partial t^2}E_X}_{\text{linear part}} \underbrace{-j\gamma\frac{8}{9}\left(|E_X|^2 + |E_Y|^2\right)E_X}_{\text{nonlinear part}}$$

$$\frac{\partial E_Y}{\partial z} = -\frac{\alpha}{2}E_Y + \frac{j\beta_2}{2}\frac{\partial^2}{\partial t^2}E_Y - j\gamma\frac{8}{9}\left(|E_X|^2 + |E_Y|^2\right)E_Y. \quad (3)$$

B. Split Step Fourier Method

The forward propagation equation described by eq. (3) can be split into its linear and nonlinear operators as

$$\frac{\partial E}{\partial z} = (\hat{D} + \hat{N})E \quad (4)$$

where $\hat{D} = -\frac{\alpha}{2} + \frac{j\beta_2}{2}\frac{\partial^2}{\partial t^2}$ is the linear component and $\hat{N} = -j\frac{8}{9}\gamma(|E_X|^2 + |E_Y|^2)$ the nonlinear one. The solution of eq. (4) reads as

$$E(z+h,t) = e^{h(\hat{D}+\hat{N})}E(z,t) \quad (5)$$

where z is the current position within the span, t is the time, and h is the step size. If h is sufficiently small, eq. (5) can be approximated by the split step Fourier method (SSFM) enabling the separation of the two operators $\hat{D}$ and $\hat{N}$ [11], yielding the solution

$$e^{h(\hat{D}+\hat{N})}E(z,t) \approx e^{h\hat{D}}e^{h\hat{N}}E(z,t). \quad (6)$$

This is equivalent to each span consisting of a cascade of linear and nonlinear parts. The SSFM algorithm forms the core of DBP as illustrated in Fig. 2, while Fig. 3 reports an example of performance of DBP applied to a 10×224 Gb/s POLMUX-16-QAM experimental setup as described in [25]: where DBP-5s refers to a DBP employing five steps per span. Clearly, the higher the number of steps considered, the better. More in detail, the linear step provides the dispersion compensation as carried out by the FDE, analytically expressed as

$$E(z+h,t) = \mathcal{F}^{-1}\{\mathcal{F}\{E(z,t)\}H(f)\}$$
$$\text{where } H(f) = e^{jh\beta_2(2\pi f)^2/2}. \quad (7)$$

The information about the accumulated dispersion to be compensated for, differently from the case with FDE, is provided by the link description.

Concerning the power dependent nonlinear mitigation this is applied on a symbol-by-symbol basis, by the following complex exponential factor

$$E(z+h,t) = E(z,t)e^{-jh\gamma|E(z,t)|^2\phi} \quad (8)$$

where $\phi \in [0,1]$ is a variable introduced to tune and optimize the nonlinear mitigation as proposed in [11]. Clearly, $\phi = 0$ implies that only standard FDE is used. To efficiently perform DBP, it is necessary to acquire accurate knowledge of all physical parameters of the transmission link. First proposals to avoid the need of a precise link description have been presented in [33], [34].

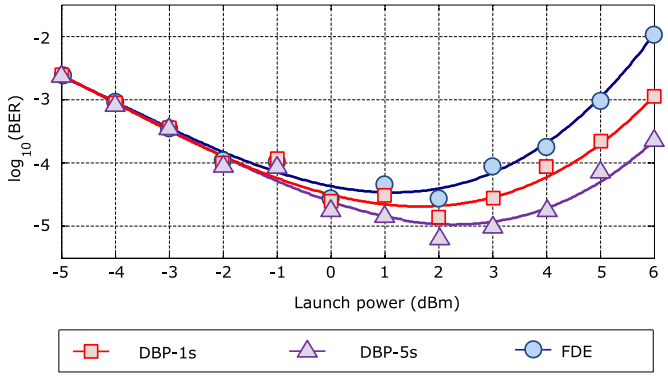

Fig. 3. $\text{Log}_{10}(\text{BER})$ as function of launch power for the experimental transmission of 10×224 Gb/s POLMUX-16-QAM channels over LA-PSCF and a NDM link as described [25].

C. Nonlinear Channel Models

The optimal value for the step size h, in terms of performance of DBP, would tend to zero. Obviously, this is unpractical because it would require an almost infinite number of steps within the SSFM, therefore we assumed $h = L_{\text{eff}}$ as proposed in [11]. Consequently, eq. (6) reads now as

$$e^{h(\hat{D}+\hat{N})}E(z+h,t) \approx e^{h\hat{D}}e^{L_{\text{eff}}\hat{N}}E(z,t) \quad (9)$$

where $L_{\text{eff}} \leq h\phi$ is the fiber effective length as defined in [6]. In [11], three different nonlinear models were described to position the linear and nonlinear blocks within a span to solve eq. (9), as shown in Fig. 4. Within the Wiener model, the linear part precedes the nonlinear, whereas in the Hammerstein it is the other way around. The union of them is named the Wiener-Hammerstein (W-H) model, which consists of three blocks. First, a linear step is performed to compensate for part of the

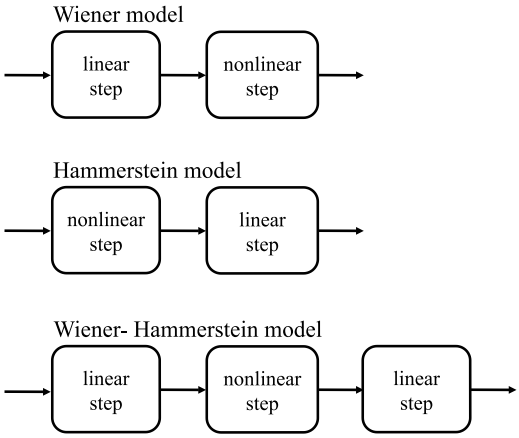

Fig. 4. Fiber nonlinear models used in the SSFM as described in [11].

accumulated dispersion, then, the nonlinear compensation is performed. At the end, the residual dispersion will be canceled by a second linear step. In this article only the W-H model is considered.

IV. Reduced Complexity Digital Back-propagation Method for NDM Links

In this section, we first want to investigate the dependence of the performance of DBP on the two dispersive linear blocks constituting the W-H model as reported in Fig. 4. Then, we will investigate the accuracy of DBP, when only a subset of the total number of spans is digitally back-propagated over a NDM link. In particular, we determine the minimum number of spans required by DBP to guarantee comparable performance to the case of complete DBP employing only one step per span confirming the results reported in [11]. The performance will be hereafter assessed in terms of *increase of optimum input power* ($\Delta P^{\text{opt}}_{\text{in,gain}}$), defined as follows

$$\Delta P^{\text{opt}}_{\text{in,gain}} = P^{\text{opt}}_{\text{TX}}(w/\text{DBP}) - P^{\text{opt}}_{TX}(w/o\ \text{DBP})$$

where $P^{\text{opt}}_{\text{TX}}(w/\text{DBP})$ is the optimal transmitted launch power[3] with DBP applied, and $P^{\text{opt}}_{\text{TX}}(w/o\,\text{DBP})$ without it (i.e., only FDE is used). The W-H model of Fig. 4, applied to NDM systems, is equivalent to a Wiener one and the linear blocks of two successive spans can be performed in a single DBP step. This does not increase the algorithm complexity, apart for an extra step required at transmitter and receiver.

Based on the results presented in [11], we optimized the length of the first (in backward propagation) dispersive block[4] of W-H as displayed in Fig. 5 assuming to perform one DBP per span. In our analyses we considered a 2×224 Gb/s POLMUX-16-QAM transmitted over 8×82 km LA-PSCF employing the setup described in [25]. The optimal dispersive length was evaluated by measuring the $\log_{10}$(BER) as function of the amount of dispersive length for different optical launch powers. We point

[3]The optimal launch power is here defined as the one that minimizes the BER of the system under test.

[4]Note that the length of the first dispersive block is equal to the total span length minus the length of the second.

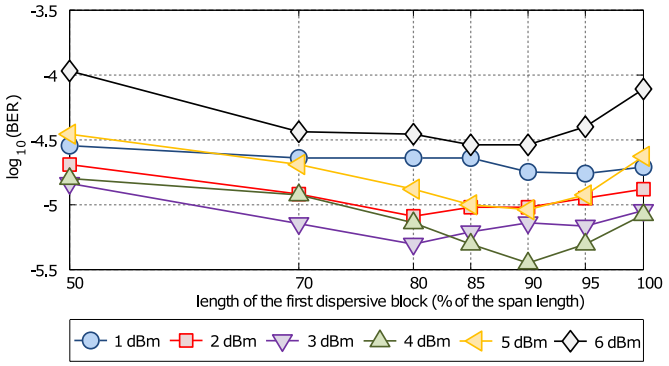

Fig. 5. Log_{10}(BER) as function of the length of the first dispersive block for the simulation of NDM transmission of 2×224 Gb/s POLMUX-16-QAM channels over LA-PSCF and NDM link.

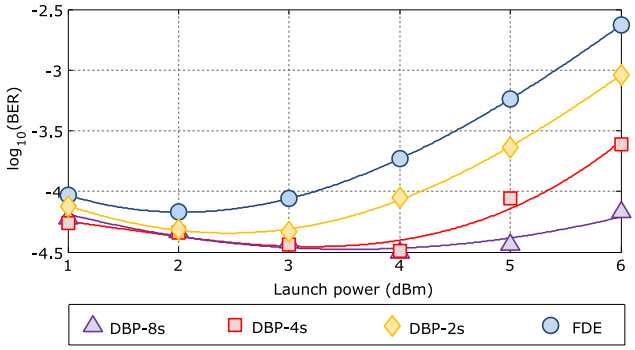

Fig. 6. Log_{10}(BER) as function of launch power for the numerical transmission of 2×224 Gb/s POLMUX-16-QAM channels over LA-PSCF and a NDM link.

out that the transmission of 2 adjacent 224 Gb/s channels as in [25] represents one of the possible solution to transmit 400 Gb/s per channel. In Fig. 5, the location of the nonlinear compensator within a DBP step is varied. If the length of the first dispersive block equaled the whole step length (i.e., 100%), this would correspond to the Wiener model. The results of Fig. 5 highlight that on average the optimal length of the first dispersion block is around 85% (as reported also in [11]). This implies that an optimization of the position of the nonlinear block enhances the algorithm performance. This observation will be later exploited to improve the performance of DBP and to enable a reduction of the number of steps without degrading the overall performance.

A. Simulations Results

In this section, we show that by employing DBP for only a subset of the total number of spans, the system performance is preserved and $\Delta P^{\text{opt}}_{\text{in,gain}}$ can be still considerably improved. Fig. 6 displays the numerical results of the transmission of 2×224 Gb/s channels over 656 km of LA-PSCF when back-propagating over 2, 4, and 8 spans[5] in a link consisting of total 8 spans.

[5]In the rest of this section, DBP-Ns means that *N* steps are back-propagated for the whole link.

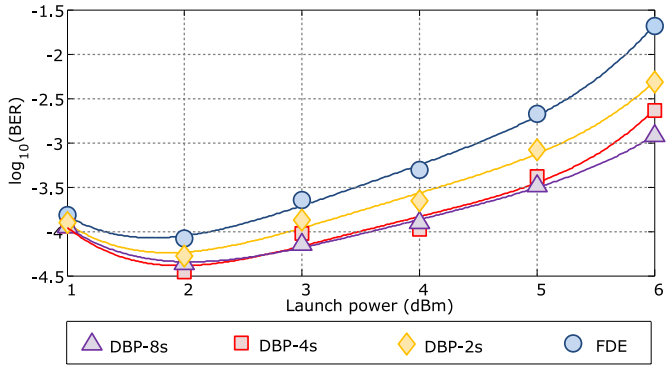

Fig. 7. Log_{10}(BER) as function of launch power for the numerical transmission of 10×224 Gb/s POLMUX-16-QAM channels over LA-PSCF and a NDM link.

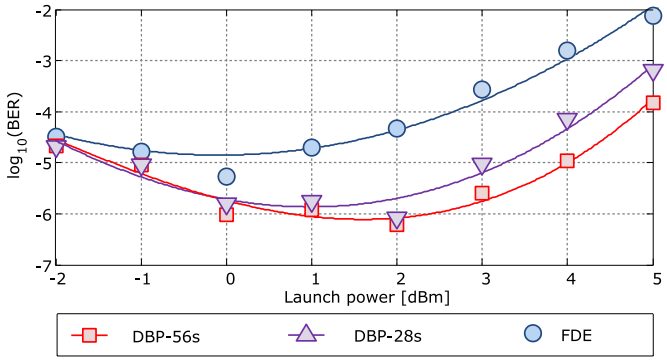

Fig. 8. Log_{10}(BER) as function of the launch power for the experimental transmission of 1×112 Gb/s POLMUX-QPSK channel over LA-PSCF and NDM system with 56 spans.

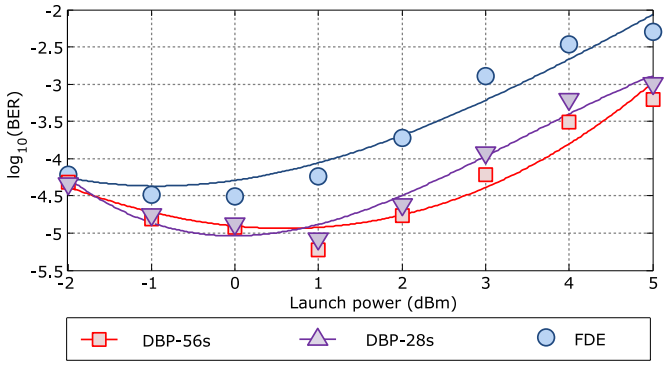

Fig. 9. Log_{10}(BER) as function of the launch power (dBm) for the experimental transmission of 11×112Gb/s POLMUX-QPSK channel over LA-PSCF and NDM system with 56 spans.

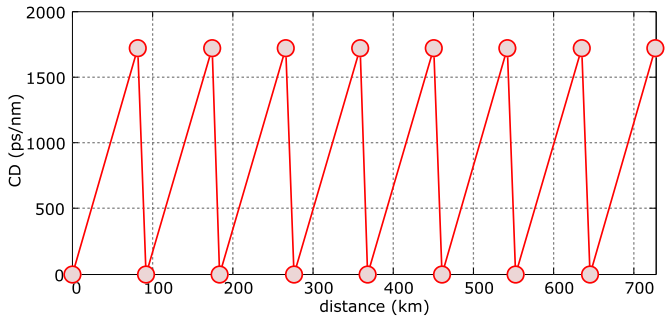

Fig. 10. Example of a fully compensated dispersion map.

From these results it is clear that the performance with respect to the complete DBP as reported in Fig. 6 is not importantly affected by back-propagating only half of the number of spans (i.e., DBP-4s, □), especially for relatively low launch powers (i.e., $P_{\mathrm{TX}} \leq 4\,\mathrm{dBm}$), since the 2 dB $\Delta P^{\mathrm{opt}}_{\mathrm{in,gain}}$ is preserved. Finally, the usage of only two steps (i.e., DBP-2s, ◇), although significantly degrading the optimal system performance, still provides a little improvement with respect to the case of FDE only. We conclude that a minimum of 4 spans (i.e. half of the total number of spans) must be back-propagated.

Fig. 7 displays $\log_{10}$(BER) results versus launch power for different number of steps of a simulated WDM transmission with 10×224 Gb/s over 656 km of LA-PSCF. The conclusions claimed for Fig. 6 are still valid, i.e., the performance of the full back-propagation and the halved one is comparable. Finally, we point out that only a minor degradation in BER and optimal launch power ($\leq$ 1 dBm) is observed, which confirms the findings of [11] .

B. Experimental Results

The concept illustrated in the previous subsection has been verified through the post-processing of experimental data as described in [26]. Here a 1×112 Gb/s POLMUX-QPSK signal has been propagated over 56 spans of LA-PSCF with a span length of 82 km. The $\log_{10}$(BER) versus P_{TX} curves displayed in Fig. 8 are fully consistent with the numerical results of Fig. 6. In particular, for $P_{\mathrm{TX}} \leq 2$ dBm, the back-propagation of only half of the total number of spans (DBP-28s, △) still provides a considerable improvement with respect to the linear equalization (i.e., FDE, ◯), preserving the 2 dBm $\Delta P^{\mathrm{opt}}_{\mathrm{in,gain}}$.

Fig. 9 shows the WDM transmission of 11×112 Gb/s POLMUX-QPSK channels over the same link, confirming the behavior observed for the single channel scenario, i.e., the $\Delta P^{\mathrm{opt}}_{\mathrm{in,gain}}$ is preserved by back-propagating only half of the spans.

V. Reduced Complexity Digital Back-propagation Method for Dispersion Managed Links

In [35], we showed that the amount of compensated dispersion within a DBP step plays a significant role in the interaction between linear and nonlinear parts within the SSFM algorithm, thus modifying the accuracy of the DBP algorithm.

If dispersion could be completely neglected (i.e., $D = 0$ ps/nm/km), the entire link would become symmetrical, with respect to SSFM. This is equivalent (if all spans are identical) to a link that could be modeled with only nonlinear steps which are compensated by a single DBP step.

In currently deployed DM links, dispersion is inline compensated through dispersion compensating fiber (DCF), and the residual amount of inline dispersion depends on the particular system design. Fig. 10, for example, illustrates a fully dispersion compensated link, where the accumulated dispersion after each span is 0 ps/nm. During the execution of SSFM, all spans

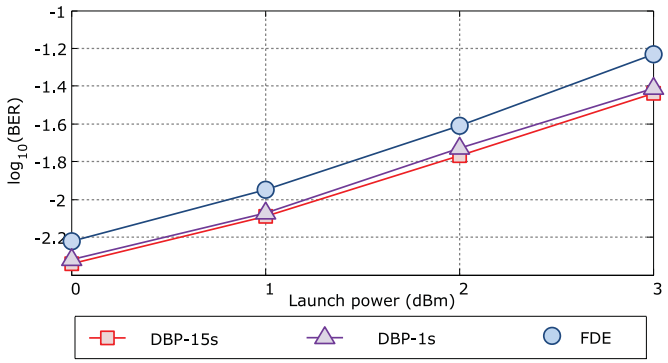

Fig. 11. Log_{10}(BER) as function of the launch power for a simulated full compensated DM link.

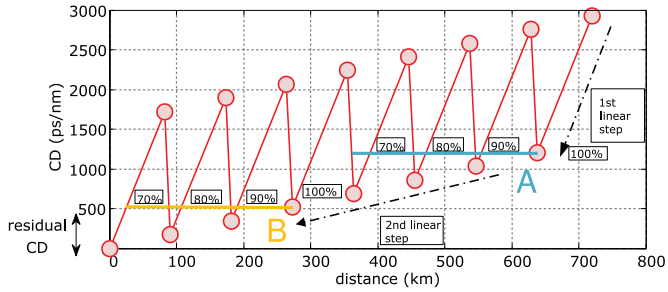

Fig. 12. Example of dispersion map with 10% under-compensation for a simulated link consisting of 8 spans SSMF and 7 DCF.

of the link displayed in Fig. 10 presenting identical dispersion profile, can be treated as a single span with equivalent length of *N times the identical spans*. This is possible because the amount of dispersion, at the beginning and the end of the span, is the same. Consequently, linear steps are not needed and only one DBP step for the entire link is required. On the other hand, if we had applied the standard DBP (including DCF), a total of $(2N-1)$ DBP steps would have been necessary, where N is the number of spans. It is worth mentioning that the nonlinearities induced by DCF can be normally neglected because of their relatively low input power and short length. Fig. 11 displays the post-processing of a simulated 2×224 Gb/s POLMUX 16-QAM channels propagated over a full inline compensated SSMF link consisting of 8 spans SSMF plus 7 spans DCF. The results with 15 and 1 DBP step are clearly comparable, even though the solution with one step DBP for the whole link considers the nonlinear effects over DCF negligible. The complexity reduction achieved by this method is of 95% with respect to the case where at least one DBP step is employed within each span. However, systems with fully inline dispersion compensation are not suitable for long-haul high data-rate transmission, since the benefit of nonlinear mitigation through the significant amount of accumulated dispersion is lost.

Fig. 12 shows a 8×82 km DM link, with a 10% under-compensation (i.e., after each span, only 90% of the accumulated dispersion is compensated). The DM link includes pre- and post-compensation, a condition that will be considered and exploited when applying DBP. Starting from the point on the right (indicated by A) and tracing the blue horizontal line towards left, a series of points over the link with the identical accumulated dispersion are identified. Similarly to the fully inline compensated links, they can be merged, thus reducing the required number of DBP steps. As it can be seen in Fig. 12, the accumulated dispersion at the point A does not correspond to the one at the beginning of the next span (in backward direction), but to an intermediate point located within the effective length L_{eff}. For the case of LA-PSCF and a span length of 82 km, $L_{\mathrm{eff}} \sim 25\,\mathrm{km}$. It has been found that the performance of backward propagation using the W-H model is optimum when the length of the first dispersive block is between 70% and 100% of the span length (see Fig. 5). This corresponds roughly to the nonlinear step being placed within L_{eff} from the end (in backward direction). (For the case of LA-PSCF and a span length of 82 km, $L_{\mathrm{eff}} \approx 25\,\mathrm{km}$ corresponds to 30%).

By referring to Fig. 12, a total of 7 spans (4 SSMF and 3 DCF) is merged and the nonlinear compensation is performed in a single step over them. Here, to further reduce the complexity, we neglected the nonlinear compensation over the DCF, since the induced nonlinearities are significantly low. In general, a lower under-compensation enables a higher complexity reduction, because more spans can be merged together. On the other hand, by doing that, a system degradation of the performance against nonlinearities is introduced, since the dispersion map is not optimal anymore. A tradeoff between complexity reduction and performance versus residual inline dispersion is therefore required. With respect to Fig. 12, the procedure followed during our post-processing his hereafter summarized:

1) The accumulated dispersion of the last span is compensated in one single linear DBP step, till the value indicated by the letter A
2) The nonlinear compensation over the last and the following 3 neighbor spans is performed by DBP.
3) Then, a second linear DBP step compensates for the accumulated dispersion from A to B, in order to keep the amount of uncompensated residual dispersion in a range between 70% to 100%
4) A second nonlinear step is applied to the last 4 spans
5) Finally, the residual linear effects are compensated for by the TDE. A side effect of our proposal is that the residual dispersion at the end of DBP is higher than the case where we employ one DBP steps per span, and consequently a higher number of taps is required by the TDE, linearly increasing the complexity. This limits the number of spans that can be actually merged and it has been taken into account during the analysis carried out in Section VI.

A. Simulation Results

Fig. 13 shows the transmission performance of 2×224 Gb/s POLMUX-16-QAM channels over 8 spans of LA-PSCF. The link is designed according to the dispersion map depicted in Fig. 12 and using the setup described in [25]. Fig. 13 highlights how similar is the performance of DBP with 15 steps (DBP-15 s, □) and with only 2 blocks of merged steps (DBP-2s, ▷), a finding that leads to a considerable complexity reduction. The

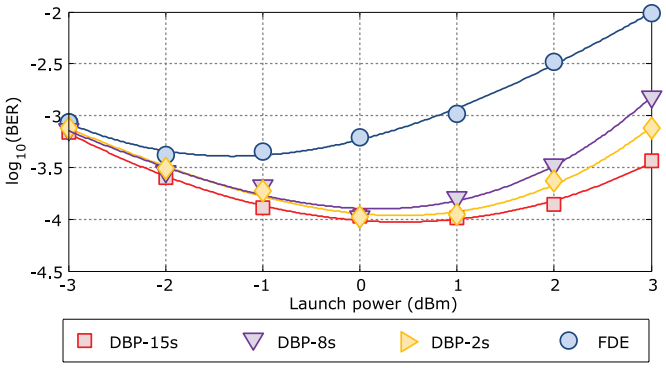

Fig. 13. Log_{10}(BER) as function of the launch power for the numerical transmission of 2×224 Gb/s POLMUX-16-QAM over LA-PSCF and DM link.

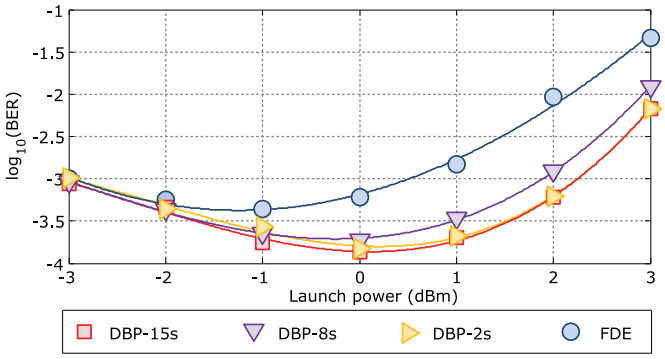

Fig. 14. Log_{10}(BER) as function of the launch power for the numerical transmission of 10×224 Gb/s POLMUX-16-QAM over LA-PSCF and with DM transmission.

result with 8 steps corresponds to the case where the nonlinear compensation in the DCF is neglected. In all cases DBP employed the same algorithm. Finally, the label FDE indicates as before the post-processing with only linear equalizer. The configuration with only 2 steps (DBP-2s, $\triangleright$) performs better than the ones with 8 steps (DBP-8s, $\triangledown$), because we know that using W-H with an optimized length improves the nonlinear compensation provided by DBP. Last but not the least, the 2 dBm of $\Delta P^{\mathrm{opt}}_{\mathrm{in,gain}}$ are preserved by using the two blocks of merged spans with respect to the case of full DBP.

This method was also verified with a 10×224 Gb/s POLMUX 16-QAM transmitting over the same setup. The results are reported in Fig. 14 and show that the 1 dB improvement in terms of $\Delta P^{\mathrm{opt}}_{\mathrm{in,gain}}$ is preserved by using the configuration with the blocks of merged spans.

B. Experimental Results

Finally, our proposal was experimentally verified by post-processing data for the WDM system as described in [4] and consisting of 10×111Gb/s POLMUX-RZ-DQPSK channels. The gross symbol rate was 27.75 Gb/s, while the net was 25 GSymbol/s and the channel spacing 50 GHz. The transmitter output signal is pre-distorted with −1530 ps/nm using DCF and launched into a recirculating loop consisting of 5×95 km SSMF. The inline dispersion under-compensation per span was −85 ps/nm, corresponding to an under-compensation of 5%.

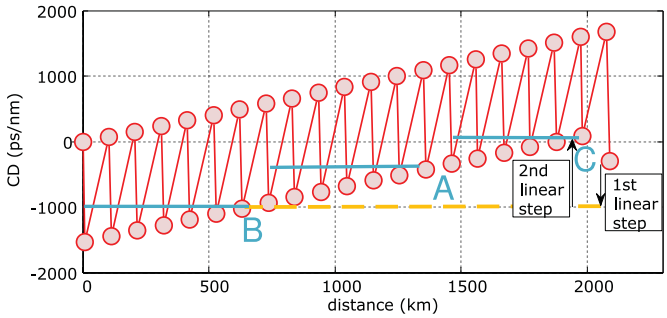

Fig. 15. Dispersion map for the experimental transmission of 11×100 Gb/s channels over 1900 km (4 loops) over DM link [4].

TABLE III
NUMBER OF REQUIRED LINEAR STEPS, NONLINEAR STEPS AND TAPS FOR EACH NUMBER OF THE LOOPS FOR THE DESCRIBED EXPERIMENT WITH DM LINK

Loops number	linear steps	nonlinear steps	TDE number of taps
3	2	2	19
4	2	3	13
5	3	4	13
6	3	4	19

Post-dispersion compensating fiber and fiber-based tunable dispersion compensation are used to set the net dispersion at the end of the link to near zero. Fig. 15 depicts the dispersion map of the described experiment for a transmission distance of 1900 km (i.e., 4 loops). The pre-compensation at the transmitter implies that the absolute value of the residual dispersion after the reduced complexity DBP is higher than the one we had in our previous simulation setup, condition that implies the usage of a larger number of taps for the TDE (i.e., the computational complexity slightly increases). Furthermore, due to the low under-compensation rate, more than 4 spans of the link can be here packed up together, leading to a consistent complexity reduction.

The residual dispersion at the end of the link is ∼300 ps/nm (point C), a value not far from the one that dispersion assumes in A (see Fig. 15). As a consequence, the linear step at the beginning of DBP can be omitted and only the nonlinear one over 6 spans is performed. Afterwards, a first DBP linear step is required to bring the accumulated dispersion down to the value of B. Once the second nonlinear step is executed over 8 spans, a last linear compensation pushes the accumulated dispersion down to 85 ps/nm, which is the value of dispersion at the beginning of the last span of the link (from a backward propagation point of view). At this point, nonlinear compensation is performed over the final 6 spans. The remaining dispersion is compensated by the TDE.

To summarize, for our considered link, consisting of 20 spans plus 21 DCF modules, only 2 linear and 3 nonlinear steps of the DBP algorithm were required. A similar procedure has been applied to the case of 3, 5 and 6 loops. Depending on the dispersion map, the number of required linear and nonlinear steps must be determined. Table III reports the requirements for each number of loops. Finally, Fig. 16 shows the $\log_{10}$(BER) results for different number of loops with the FDE, the standard DBP algorithm and our modified DBP with reduced complexity

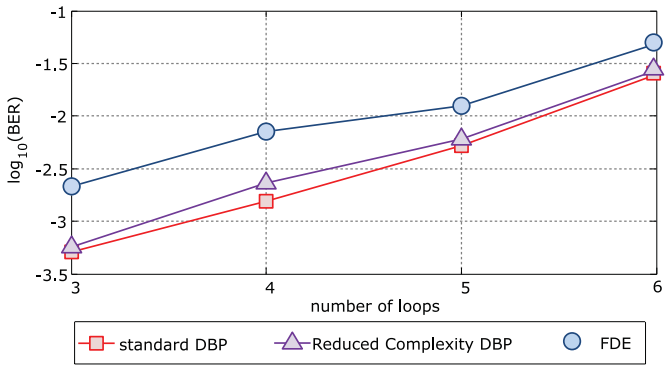

Fig. 16. $\mathrm{Log}_{10}(\mathrm{BER})$ as function of the number of loops for FDE, standard DBP and reduced complexity DBP at $P_{\mathrm{TX}} = 0$ dBm with a DM link as described in [4].

(all results are with $P_{\mathrm{TX}} = 0$ dBm). Although the system was operating in weak nonlinear regime, a clear improvement provided by DBP is observed. In this last analysis the benefit was quantified by measuring the gain in terms of number of loops. Clearly, the performance of the reduced complexity DBP is comparable to the one of the standard DBP. The maximum distance at $\log_{10}(\mathrm{BER}) = -2.4$ (i.e., $\mathrm{BER} = 3.8 \cdot 10^{-3}$, a standard value for hard decision FEC) is increased by about 500 km compared with the case of FDE only. This validates the results obtained by the post-processing of the numerical simulations of Section V-A.

VI. Complexity Analysis

The goal of this section is to discuss the hardware complexity required by the method reported in Section V. In particular, based on the calculations carried out in [36] concerning FDE and TDE, we will compare the amount of complex multiplication per bit needed by DBP with our proposal against linear FDE and a standard realization of DBP.

In [36], it has been demonstrated that among linear equalizers, FDE is less complex than TDE as long as the channel memory exceeds a certain length. Nevertheless, the joint usage of them is a must for modern DSP-CRX because FDE compensates for the bulk dispersion; while TDE cancels the remaining residual dispersion, demultiplexes the signal and compensates for other linear effects such as PMD and PDL.

FDE removes dispersion by multiplying the signal with the inverse of the dispersion transfer function as described by eq. (7). The amount of the accumulated dispersion is estimated after the transmission, and based on that, the FDE dynamically adapts its parameters as reported in [27]. In [37] the computational complexity of the FDE C_{FDE} has been calculated in terms of number of complex multiplication per transmitted bit, and reads as

$$C_{\mathrm{FDE}} = \frac{N[\log_2(N)+1]n}{(N - N_D + 1)\log_2(M)} \tag{10}$$

where N is the FFT size, M is the order of the modulation format (e.g. 4 for QPSK, 16 for 16-QAM), n the oversampling ratio, and $N_D = n\tau_D/T$, where τ_D corresponds to the dispersive channel impulse response and T is the symbol duration. A detailed derivation of the formulas can be found in [37]. On the other hand, TDE mitigated propagation effects through coefficient adaptation and its complexity C_{TDE} is also estimated in [37] and reads as

$$C_{\mathrm{TDE}} = \frac{4N_{\mathrm{taps}}}{\log_2(M)} \tag{11}$$

where N_{taps} is the number of taps needed by TDE. Summing up eqs. (10) and (11), the final expression for the linear equalizer complexity C_{LE} is determined as follows

$$C_{\mathrm{LE}} = \frac{N[\log_2(N)+1]n}{(N - N_D + 1)\log_2(M)} + \frac{4N_{\mathrm{taps}}}{\log_2(M)}\,. \tag{12}$$

However, the optimal FFT-size depends on the amount of dispersion to be compensated for as described in eq. (10), and this value is different between NDM and DM links. For instance, in case of NDM links, the accumulated dispersion within one span is considerably low compared to the overall amount, therefore the FFT-size needed by the FDE at the receiver is considerably larger compared to the one of the linear DBP stage at each span. On the other hand, in DM links, both compensation techniques have almost the same complexity since the dispersion accumulated over one span is comparable to the one at the receiver. Concerning the DBP for the linear part, no dispersion estimation is required because we assume a full knowledge of the transmission link, while the nonlinear one, performed in the time domain, reveals after a closer look at the Manakov equation that only one complex multiplication per sample is needed. Last but not the least, after the linear and nonlinear steps of the DBP, the TDE is still required. The total complexity of one DBP stage for the DM analyzed in Section V finally reads as

$$C_{\mathrm{DBP}} = \frac{N[\log_2(N)+1]n}{(N - N_D + 1)\log_2(M)} + n. \tag{13}$$

More precisely, for the case of the previous inline compensated link with 10% under-compensation and assuming to merge 4 spans together, we back-propagate only $N_{\mathrm{spans}}/4$, while the standard DBP (including DCF) would have required $(2N_{\mathrm{spans}} - 1)$ DBP steps. In addition, the proposed method for DM link will employ a slightly higher number of taps within the TDE to compensate for the higher amount residual dispersion. Mathematically this is expressed as

$$C_{\mathrm{standardDBP}} = N_{\mathrm{steps}} \cdot C_{\mathrm{DBP}} + C_{\mathrm{TDE}}^{n_{\mathrm{taps}}}$$

$$C_{\mathrm{reducedDBP}} = \left(\frac{N_{\mathrm{steps}}+1}{8}\right) C_{\mathrm{DBP}} + C_{\mathrm{TDE}}^{n_{\mathrm{taps}}+n'_{\mathrm{taps}}}$$

where N_{steps} is the number of DBP steps over the whole link and n'_{taps} is the additional number of taps added to TDE because of the remaining dispersion after the reduced complexity DBP.

Fig. 17 displays the number of complex multiplications per transmitted bit for the case of LE, standard DBP and reduced complexity DBP. We consider in Fig. 17 the scenario described in Section V-A. The values here presented are for an FFT size of 256, 13 taps for the LE and the standard DBP. The residual dispersion after the DBP for the map shown in Fig. 12 needs 6 taps more (i.e., 19 taps) than the case with standard DBP. Fig. 17

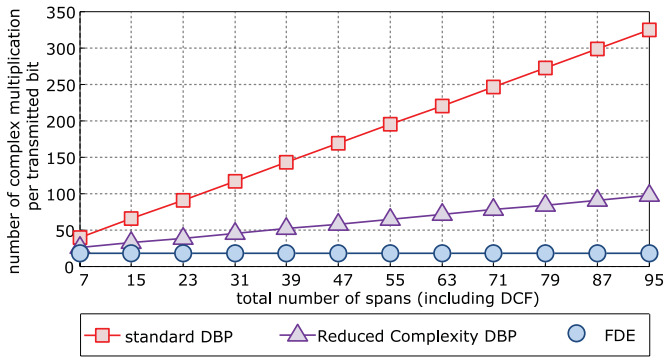

Fig. 17. Complexity of a LE, standard DBP and reduced complexity DBP as function of the total number of spans for a simulated DM link.

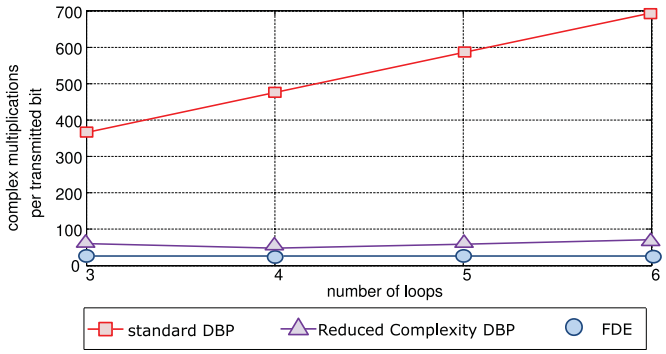

Fig. 18. Complexity of an LE, standard and reduced complexity DBP as function of the number of loops for the described experiment with DM link.

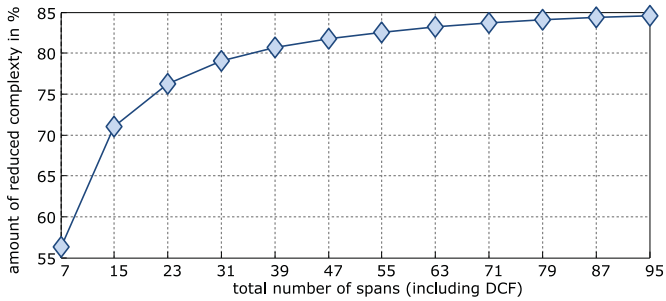

Fig. 19. Reduction of the complexity of the reduced complexity BP regarding the standard BP for the previous described link.

shows that the reduced complexity DBP requires more complex multiplications per transmitted bit than the LE, but it dramatically reduces the computational complexity in comparison with the standard DBP algorithm. The complexity reduction, defined as the fraction of the complex multiplications saved by the reduced complexity DBP and the number of complex multiplications needed by the standard DBP is of about 70%.

Fig. 18 shows the complexity of the LE, reduced complexity DBP and standard DBP for the experiment described before. In this experiment, the accumulated dispersion at the end of the link was small enough to be recovered by a TDE only. Fig. 18 reports the number of complex multiplications per transmitted bit as function of the number of loops. Clearly, the complexity of the standard DBP is considerably larger than the one of the reduced DBP, which is in the same range of the one of the LE. Finally, Fig. 19 displays the complexity reduction as function of the total number of spans (including DCF) for the case of the experiment reported in Section V-B. For long transmission distances, i.e., a high number of spans, the complexity reduction saturates at 85%, which represents a significant gain in terms of hardware complexity.

VII. Conclusion

In this study, we proposed two methods for managed and NDM optical communication systems to decrease the hardware computational complexity required by the DBP algorithm. The two proposals have been verified by post-processing simulated and experimental data.

For the NDM scenario, we confirmed, and further investigated, the scenarios presented in [11], showing that the joint usage of W-H model and a halved back-propagation besides reducing the required hardware resources by $\sim 50\%$, preserves the performance improvement obtained by employing a full DBP (i.e., one step per each span).

Concerning the DM scenario, the design of the dispersion map has been exploited to lower the number of steps required by DBP while keeping his optimal performance in terms of $\Delta P_{\mathrm{in,gain}}^{\mathrm{opt}}$. Our analysis considered two typical dispersion managed optical links with 10% and 5% under-compensation, respectively. In both cases, we reported a complexity reduction as high as 85%.

For the case of a DM link the reduction in terms of hardware requirements lowers the DBP computation complexity to an amount comparable to the one of linear equalization, paving the way for the realization of real-time chip employing DBP.

Acknowledgment

This work was partially supported by the FP-7 IDEALIST project under grant agreement number 317999. A. Napoli would like to thank Dr. M. S. Alfiad for the fruitful discussions.

References

[1] Amsterdam Data Exchange. [Online]. Available: http://www.ams-ix.net/
[2] (2013).White paper, "Cisco Visual Networking Index: Forecast and Methodology, 20122017," [Online]. Available:http:// www.cisco.com
[3] D. van den Borne, "Robust optical transmission systems: modulation and equalization," Ph.D. thesis, Tech. Univ. Eindhoven, Eindhoven, The Netherlands, 2008.
[4] C. R. S. Fludger, T. Duthel, D. van den Borne, C. Schulien, E. D. Schmidt, T. Wuth, J. Geyer, E. De Man, G. D. Khoe, and H. de Waardt, "Coherent equalization and POLMUX-RZ-DQPSK for robust 100-GE transmission," *IEEE / OSA J. Lightw. Technol.*, vol. 26, no. 1, pp. 64–72, Jan. 2008.
[5] M. S. Alfiad, "Multilevel modulation formats for robust long-haul high capacity transmission," Ph.D. thesis, Tech. Univ. Eindhoven, Eindhoven, The Netherlands, 2011.
[6] G. Agrawal, *Lightwave Technology: Telecommunication Systems*. New York, NY, USA: Wiley, 2005.
[7] Y. Gao, F. Zhang, L. Dou, Z. Chen, and A. Xu, "Intra-channel nonlinearities mitigation in pseudo-linear coherent QPSK transmission systems via nonlinear electrical equalizer," *Opt. Commun.*, vol. 282, no. 12, pp. 2421–2425, Jun. 2009.
[8] S. Randel, S. Adhikari, and S. L. Jansen, "Analysis of RF-Pilot-based phase noise compensation for coherent optical OFDM systems," *IEEE Photon. Technol. Lett.*, vol. 22, no. 17, pp. 1288–1290, Aug. 2010.
[9] A. Diaz, A. Napoli, S. Adhikari, Z. Maalej, A. Lobato, M. Kuschnerov, and J. Prat, "Analysis of back-propagation and RF pilot-tone based nonlinearity compensation for a 9×224 Gb/s POLMUX 16-QAM system," in *Proc. Opt. Fiber Conf*, 2012, Paper OTh3C.5,

[10] X. Liu, A. R. Chraplyvy, P. J. Winzer, R. W. Tkach, and S. Chandrasekhar, "Phase-conjugated twin waves for communication beyond the Kerr nonlinearity limit," *Nat. Photon.,* vol. 7, pp. 560–568, 2013.

[11] D. S. Millar, S. Makovejs, C. Behrens, S. Hellerbrand, R. I. Killey, P. Bayvel, and S. J. Savory, "Mitigation of fiber nonlinearity using a digital coherent receiver," *IEEE J. Sel. Topics Quantum Electron.*, vol. 16, no. 5, pp. 1217–1226, Oct. 2010.

[12] E. Ip and J. M. Kahn, "Compensation of dispersion and nonlinear impairments using digital backpropagation," *IEEE / OSA J. Lightw. Technol.*, vol. 26, no. 20, pp. 3416–3425, Oct. 2008.

[13] F. Yaman and G. Li, "Nonlinear impairment compensation for polarization-division multiplexed WDM transmission using digital backward propagation," *IEEE Photon. J.*, vol. 1, no. 2, pp. 144–152, Aug. 2009.

[14] D. Rafique, J. Zhao, and A. D. Ellis, "Performance Improvement by Fibre Nonlinearity Compensation in 112 Gb/s PM M-ary QAM," in *Proc. Opt. Fiber Conf. (OFC)*, 2011, paper OWO6.

[15] D. Rafique and A. D. Ellis, "Nonlinear penalties in dynamic optical networks employing autonomous transponders," *IEEE Photonics Technol. Lett.*, vol. 23, no. 17, pp. 1213–1215, Sep. 2011.

[16] D. Rafique and A. D. Ellis, "Nonlinear and ROADM induced penalties in 28 GBaud dynamic optical mesh networks employing electronic signal processing," *OSA Opt. Exp.*, vol. 19, no. 18, pp. 16739–16748, 2011.

[17] D. van den Borne, V. A. J. M. Sleiffer, M. S. Alfiad, S. L. Jansen, and T. Wuth, "POLMUX-QPSK modulation and coherent detection: The challenge of long-haul 100G transmission," in *Proc. 35th Eur. Conf. Opt. Commun.*, 2009, pp. 1–4.

[18] M. S. Alfiad, M. Kuschnerov, T. Wuth, T. J. Xia, G. Wellbrock, E. D. Schmidt, D. van den Borne, B. Spinnler, C. J. Weiske, E. de Man, A. Napoli, M. Finkenzeller, S. Spaelter, M. Rehman, J. Behel, M. Chbat, J. Stachowiak, D. Peterson, W. Lee, M. Pollock, B. Basch, D. Chen, M. Freiberger, B. Lankl, and H. de Waardt, "111-Gb/s Transmission over 1040-km field-deployed fiber with 10G/40G neighbors," *IEEE Photon. Technol. Lett.*, vol. 21, no. 10, May 2009, pp. 615–617

[19] M. S. Alfiad, D. van den Borne, S. L. Jansen, T. Wuth, M. Kuschnerov, G. Grosso, A. Napoli, and H. de Waardt, "A comparison of electrical and optical dispersion compensation for 111-Gb/s POLMUX-RZ-DQPSK, " *IEEE / OSA J. Lightw. Technol.*, vol. 27, no. 16, Aug. 15, 2009.

[20] D. Rafique, J. Zhao, and A. D. Ellis, "Digital back-propagation for spectrally efficient WDM 112 Gbit/s PM m-ary QAM transmission," *OSA Opt. Exp.*, vol. 19, no. 6, pp. 5219–5224, 2011.

[21] L. Li, Z. Tao, L. Dou, W. Yan, S. Oda, T. Tanimura, T. Hoshida, and J. C. Rasmussen, "Implementation efficient nonlinear equalizer based on correlated digital backpropagation," in *Proc. Opt. Fiber Conf.*, 2009, Paper OWW3, .

[22] D. Rafique, M. Mussolin, M. Forzati, J. Mårtensson, M. N. Chugtai, and A. D. Ellis, "Compensation of intra-channel nonlinear fibre impairments using simplified digital backpropagation algorithm," in *Proc. OSA Opt. Exp.*, 2011, vol. 19, no. 10, pp. 9453–9460.

[23] E. Ip, N. Bai, and T. Wang, "Complexity versus performance tradeoff for fiber nonlinearity compensation using frequency-shaped, multi-subband backpropagation," in *Proc. Opt. Fiber Conf. (OFC)*, 2011, Paper OThF4.

[24] V. A. J. M. Sleiffer, D. van den Borne, M. Kuschnerov, V. Veljanovski, M. Hirano, Y. Yamamoto, T. Sasaki, S. L. Jansen, and H. de Waardt, "A comparison between SSMF and large-Aeff pure-silica core fiber for ultra long-haul 100G transmission," in *Proc. 37th Eur. Conf. Opt. Commun.*, 2011, Paper Mo.2.B.

[25] V. Sleiffer, M. Alfiad, D. van den Borne, M. Kuschneorv, V. Veljanovski, M. Hirano, Y. Yamamoto, T. Sasaki, S. Jansen, T. Wuth, and H. de Waardt, "10×224-Gb/s POLMUX-16QAM transmission over 656 km of Large-A_{eff} PSCF with a spectral effciency of 5.6 b/s/Hz," *IEEE Photon. Technol. Lett.*, vol. 23, no. 20, pp. 1427–1429, Oct. 2011.

[26] V. A. J. M. Sleiffer, Z. Maalej, D. van den Borne, M. Kuschnerov, V. Veljanovski, M. Hirano, Y. Yamamoto, T. Sasaki, S. L. Jansen, A. Napoli, and H. de Waardt, "A comparison between SSMF and large-Aeff Pure-Silica core fiber for Ultra Long-Haul 100 G transmission," *OSA Opt. Exp.*, vol. 19, no. 26, pp. B710–B715, 2011.

[27] M. Kuschnerov, F. N. Hauske, K. Piyawanno, B. Spinnler, M. S. Alfiad, Antonio Napoli, and B. Lankl, "DSP for Coherent Single-Carrier Receivers," *IEEE / OSA J. Lightw. Technol.*, vol. 27, no. 16, pp. 3614–3622, Aug. 2009.

[28] M. Kuschnerov, F.N. Hauske, K. Piyawanno, B. Spinnler, A. Napoli, and B. Lankl, "Adaptive chromatic dispersion equalization for non-dispersion managed coherent systems," in *Proc. Opt. Fiber Conf. (OFC)*, 2009, Paper OMT1.

[29] D. Godard, "Self-Recovering equalizationand carrier tracking in two-dimensional data communication systems," *IEEE Trans. Commun.*, vol. COM-28, no. 11, pp. 1867–1875, Nov. 1980.

[30] S. J. Savory, "Digital filters for coherent optical receivers," *OSA Opt. Exp.*, vol. 16, no. 2, pp. 804–817, 2008.

[31] A. Viterbi and A. Viterbi, "Nonlinear estimation of PSK-modulated carrier phase with application to burst digital transmission," *IEEE Trans. Inf. Theory*, vol. IT-29, no. 4, pp. 543–551, Jul. 1983.

[32] A. H. Gnauck, P. J. Winzer, S. Chandrasekhar, X. Liu, B. Zhu, and D.W. Peckham,Spectrally efficient long-haul WDM transmission using 224-GB/s polarization-multiplexed 16-QAM, *IEEE / OSA J. Lightw. Technol.*, vol. 29, no. 4, pp. 373–377, Feb. 2011.

[33] T. Tanimura, T. Hoshida, T. Tanaka, L. Li, S. Oda, H. Nakashima, Z. Tao, and J. C. Rasmussen, "Semi-blind nonlinear equalization in coherent multi-span transmission system with inhomogeneous span parameters," in *Proc. Opt. Fiber Conf.*, 2010, Paper OMR6.

[34] C.-Y. Lin, A. Napoli, B. Spinnler, V. Sleiffer, D. Rafique, M. Kuschnerov, M. Bohn, and B. Schmauss, "Adaptive digital back-propagation for optical communication systems," in *Proc. Opt. Fiber Conf.*, 2014, to be published.

[35] Z. Maalej, V. A. J. M. Sleiffer, E. Timmers, A. Napoli, M. Kuschnerov, B. Spinnler, and N. Hanik, "Reduced complexity back-propagation for optical communication systems," in *Proc. IEEE Photon. Conf.*, 2011, pp. 692–693.

[36] N. Benvenuto and G. Cherubini, *Algorithms for Communications Systems and their Applications*. Hoboken, NJ, USA: Wiley, 2002.

[37] B. Spinnler, "Equalizer design and complexity for digital coherent receivers," *IEEE J. Sel. Topics Quantum Electron.*, vol. 16, no. 5, pp. 1180–1192, Sep./Oct. 2010.

Antonio Napoli received the Masters and Ph.D. degrees in electronics engineering from Politecnico di Torino in 2002 and 2006, respectively. He was a Visiting Student at the Technische Universität Wien (2001), a Visiting Researcher at Universitat Politècnica de Catalunya in Barcelona (2004) and at University College London, U.K. (2005).

In 2006, he joined Siemens COM, where he worked on EDFA transient suppression and DSP for long-haul optical networks. In 2007, he joined Nokia Siemens Networks, where he worked on optical transmission up to 400 Gb/s. He has been with Coriant since 2013, where is leading a work-package on data plane within the EU FP-7 IDEALIST project. He regularly supervises students and teaches at several universities. His research interests include DSP and advanced modulation formats for long-haul systems.

Dr. Napoli is a (co)author of more than 70 peer-reviewed papers and conference contributions, and six patents.

Zied Maalej studied electrical engineering at the Munich University of Technology. After a 3 months internship at Nokia Siemens Networks (NSN) in Munich, he received the M.S. thesis within the optical communications Department of NSN. He is now working in the planning department of Vodafone Germany.

Vincent A. J. M. Sleiffer (S'09) was born in Arnhem, The Netherlands. He received the B. Sc. degree in electrical engineering and the M.Sc. degree in broadband telecommunication technologies from the University of Technology Eindhoven, Eindhoven, The Netherlands, in 2007 and 2010, respectively. He is currently working toward th Ph.D. degree, studying high capacity next-generation long-haul transmission systems at the University of Technology Eindhoven in collaboration with Coriant R&D GmbH. Munich. His research is mainly carried out in Munich. His research interests include generation of higher order modulation formats and mode division multiplexing, and combining the two to achieve large capacity transmission using novel fiber types.

Mr. Sleiffer was one of the winners of the IEEE Photonics Society Graduate Student Fellowship in 2013. He is student member of the Optical Society of America (OSA) and is a (co)author of more than 60 papers and several patents in the field of optical communication.

Maxim Kuschnerov graduated from the Technical University of Munich in 2006, and the Ph.D. degree in electrical engineering from the University of the Federal Armed Forces, Munich, Germany, in 2011. His Ph.D. research was conducted in collaboration with Nokia Siemens Networks in Munich focusing on the development of digital signal processing algorithms for optic coherent systems. In 2010, he joined NSN full time, focusing on the development of 100 Gb/s transponders and beyond. He has authored and co-authored more than 100 peer-reviewed papers and conference contributions. In 2009, he received the NSN quality award for innovation. Currently, he leads the system trial work package of the Modegap project, focusing on space division multiplexing over multi-mode fibres.

Danish Rafique received the B.Sc. degree from, FAST-NU, Pakistan, in 2007, the M.Sc. KTH, Sweden, in 2009, and the Ph.D. degree from Tyndall National Institute, University College Cork, Ireland, in 2012, all in electrical engineering. He published more than 34 articles and was a semifinalist in the OFC Best Student Paper Competition (in 2011 and 2012). Currently, he is pursuing a career with R&D Labs of Coriant GmbH, Germany, where he is working on next-generation transponder solutions involving flex-grid networks. His research interests include nonlinear effects in fiber, DSP, and flex-grid optical networks. He is a Reviewer for IEEE PHOTONICS TECHNOLOGY LETTERS, IEEE JOURNAL OF LIGHTWAVE TECHNOLOGY, and OSA OE.

Erik Timmers did an internship on back-propagation at Nokia Siemens Networks in 2010. After graduation, he founded EasyGIS, a company exercising in the field of geographical information systems.

Bernhard Spinnler received the Dipl.-Ing. degree in communications engineering and the Dr.-Ing. degree from the University of Erlangen-Nürnberg, Germany, in 1994 and 1997, respectively. Since 1997, he has worked on low-complexity modem design of wireless radio relay systems at Siemens AG, Information and Communication Networks. In 2002, he joined the Optical Networks Group, Siemens Corporate Technology, which later became Nokia Siemens Networks. He has been with Coriant since 2013, where he is working on robust and tolerant design of optical communications systems. His research interests include advanced modulation and equalization for single and multicarrier systems.

Talha Rahman was born in Lahore, Pakistan, on the 15th of September 1985. He received the B.S. degree in communication systems engineering from the Institute of Space Technology Islamabad in 2007. and the Master's (with Hons.) in advanced optical technologies from the FAU Erlangen-Nuremberg. He is currently working toward the Ph. D. degree with the collaboration of TU Eindhoven and Coriant GmbH. His is currently in Munich, Germany, where he conducts his doctoral research on high-data rate, capacity efficient flexible optical transponders in the R&D department of Coriant GmbH.

Leonardo Didier Coelho (S'09–M'12) received the B.Sc. degree in electrical engineering in 2003 from the Universidade Federal de Pernambuco, Recife, Brazil, and the M.Sc. and Dr.-Ing. degrees in 2005 and 2010, respectively, both from the Technische Universität München, Munich, Germany. In his Master's Thesis and Doctoral Dissertation he conducted research on modeling, simulation, and optimization of optical communication systems using advanced modulation formats. In 2006 and 2007, he worked on nonlinear phase noise in phase-modulated optical communication systems at the Heinrich-Hertz-Institute in Berlin. He spent the summer of 2009 at the Department of Photonics Engineering, Technical University of Denmark, as a Visiting Researcher working on fiber-based optical parametric amplifiers. Since 2011, he has been with Coriant R&D GmbH (formerly part of Nokia Siemens Networks) in Munich, Germany. His main research interests include simulation and optimization of optical communication systems, transmitter and receiver modeling for new modulation formats, optical amplification, and nonlinear signal propagation in fiber-optic transmission systems. Dr. Coelho received the Bund der Freunde der TU München Award for Outstanding Doctoral Thesis in electrical engineering in 2011. He has published several refereed papers in journals and peer reviewed conferences and is the inventor of two patents.

Norbert Hanik received the Dipl.-Ing. degree in electrical engineering from the Technische Universität München (TUM), with a thesis on digital spread spectrum systems.

From 1989 to 1995, he was a Research Associate at the Institute for Telecommunications of TUM, where he worked in the field of Optical Communications. In 1995, he received the Dr.-Ing. degree with a thesis on non-linear effects in optical signal transmission.

From 1995 to 2004, he was with the Technologiezentrum of Deutsche Telekom, heading the research group "System Concepts of Photonic Networks." From January to March 2002, he was engaged as a Visiting Professor at the Research Center COM, Technical University of Denmark, Copenhagen. During his work he contributed to a multitude of national and international R&D-projects, both as a Scientist and Project Leader.

As of April 2004, Dr. Hanik holds an Associate Professorship at TUM in the field of wired and optical signal transmission. His primary research interests include physical design, optimization, operation and management of optical networks.